https://doi.org/10.20965/jrm.2014.p0331

Paper:

Robust Hybrid Control for Two-Dimensional Handheld Micromanipulator

Sungwan Boksuwan*, Taworn Benjanarasuth, Chisato Kanamori*, and Hisayuki Aoyama***

*Department of Mechanical Engineering and Intelligent Systems, The University of Electro-Communications
1-5-1 Chofugaoka, Chofu, Tokyo 182-8585, Japan
E-mail: nybao@hotmail.com, {kanamori, aoyama}@mce.uec.ac.jp
**Faculty of Engineering, King Mongkut's Institute of Technology Ladkrabang
1 Chalongkrung Soi 1, Ladkrabang District, Bangkok, Thailand
E-mail: kbtaworn@kmitl.ac.th

[Received October 7, 2013; accepted March 24, 2014]

This paper proposes a two-dimensional handheld micromanipulator oriented toward bio cell handling. The micromanipulator consists of two flexible links, each of which is constructed with a parallel beam structure. Electric coils and permanent magnets are used to produce an actuator to form double drivers. An explicit model predictive control combined with a PID controller called a robust hybrid control is proposed not only to achieve robust tracking performance, but also to dampen the vibration of the mechanism. The experimental results are compared to results from a standard PID controller to investigate the effectiveness of the micromanipulator.

Keywords: handheld micromanipulator, parallel beam structure, explicit MPC, PID controller

1. Introduction

A micromanipulator is a tool that enables the operator to physically interact with a sample, such as a bio cell, at or beyond the threshold of human dexterity. Typical applications of micromanipulators can be classified into three platforms. The first micromanipulation system is called a master-slave robot [1, 2], mainly used for microsurgeries. The second system is referred to as a steadhand robotic system [3, 4], used in both microsurgeries and cell manipulations. The last micromanipulator, an active handheld micromanipulator, is the subject of this paper. The first handheld instrument was introduced in [5] to reduce cost and to increase the flexibility and comfort of usage. With microtechnologies, active handheld micromanipulators [6–9] have been developed for microsurgery and cell manipulation. Such manipulators are composed of piezoelectric actuators which require high voltage. In addition, the piezoelectric actuators inherently have hysteresis and nonlinearity characteristics. The design becomes complicated as a control system design because such characteristics result in complexity in terms of mathematical description. Although a dynamic behavior can be approximated as a linear time-invariant system, the resulting mathematical model is of a high order with delays which limit the achievable performances [10]. An alternative micro-actuator with simple dynamic behavior will be considered.

A manipulator with multiple flexible links, each of which consists of parallel beams, was studied in [11]. In that work, a flexible link was designed to minimize the effects of a rigid load in order to obtain decoupling links. The work presented several advantages of the parallel beam structure. In other interesting works [12] and [13], the parallel beam structure was used as a gyroscope sensor in which the effects of interference caused by imperfect fabrication or different mass between two links were discussed and softened with both passive and active strategies. The paper indicated that a control mechanism was required to handle such interference.

Recently, an advanced control method called Model Predictive Control (MPC) [14–19] has established itself in the community of industrial applications such as building controls [20, 21], power electric systems [22, 23] and automotive control systems [24]. Additionally, the model predictive control has been utilized to soften a vibration in a flexible mechanism [25–28]. In the MPC framework, a control problem was formulated as a finite-horizon open-loop optimal control problem. The optimal solution turned out to be the optimal control signal of the system at each sampling instant. Basically, the optimal policy for operating the system could come from two main paradigms. The first was called on-line optimizing control. In it, the sequence of an optimal input is obtained by solving the optimization problem with new measurements at each sampling. The first entry of the optimal sequence is applied to the system while the others are all discarded. In the next sampling, all computational processes are repeated. The second is referred to as off-line optimizing control. In it, the optimal control law is explicitly computed at the outset. This approach is also called explicit model predictive control [29], or EMPC. In addition, both paradigms rely on a state feedback control scheme. Therefore, the well-known Kalman filter is frequently used to estimate such state variables.

Fig. 1. The concept of a handheld micromanipulator.

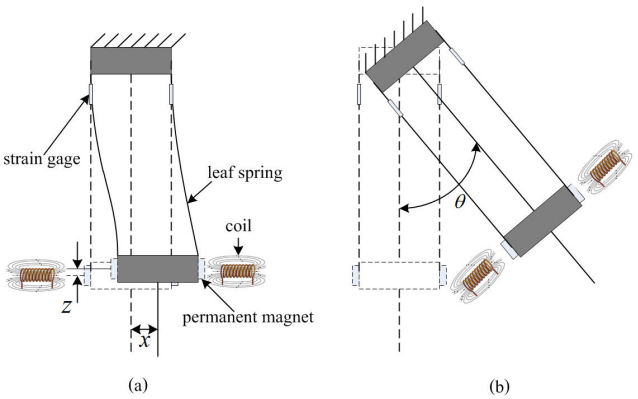

Fig. 2. Schematic of a flexible link.

In this paper, a two-dimensional handheld micromanipulator along x- and y- axes is proposed to operate on a micro scale. The operation of the handheld micromanipulator is conceptually shown in **Fig. 1**. The micromanipulator position is controlled by the user's hand, whereas the needle is automatically steered to accomplish micromanipulations with the help of the additional sensors, such as a microscope. The handheld micromanipulator in **Fig. 1** actually requires the z-axis. However, this paper focuses initially on the tracking performance along the x- and y-axes, whereas the z-axis and disturbance, which is the fluctuation caused by the user's hand, are both considered to be future work.

In the actual primary test, it was found that fluctuation in the manipulator's end position was mostly less than 100 μm during the first three seconds. Therefore, we set the working range as ± 50 μm under the condition of short operation time as the primary goal of this system. The main objectives and features of the proposed manipulator are as follows.

1) 100 μm^2 working range in the xy-plane with 1 μm resolution on each axis.
2) Simple structure and fabrication to achieve a low order mathematical model and decoupling behavior.
3) Simple driving mechanism in order to obtain a linear behavior and to avoid hysteresis.
4) Optimal robust reference tracking performance in large working range of a holding angle.
5) Incorporation of system constraints and imperfect fabrications in the controller synthesis in order to eliminate external feedforward paths that are sensitive to parameter variations.

With respect to the existing literature, the main contribution of this paper is the presentation of a design for new handheld micromanipulator, one simple in structure and fabrication in order to achieve robust tracking performance by means of the robust hybrid control.

2. Manipulator Design

2.1. Mechanical Structure

The micromanipulator consists of two cascaded, flexible links. They are connected in such a way that the first and second links are arranged to move along the y-axis and x-axis, respectively. The schematic structure of the flexible link is shown in **Fig. 2**, which shows how the parallel beams, or leaf springs, are utilized as the movement mechanism. For actuators, the combination of permanent magnets hung on the moving part and electric coils fixed on the stationary frame is utilized because such a mechanism offers a simple and linear relation of an electrical force and a voltage in a specified working range. Since the proposed micromanipulator itself has a flexible structure, the driving mechanism requires little force, i.e., low voltage and current. In addition, dynamic behavior is simple in a working range. The proposed micromanipulator structure has the following significant features.

1) The tip and base of each link move in parallel.
2) The links do not interfere with each other.
3) Because of the flexible structure, little force is required.

The decoupling feature is crucial in a control design of the handheld micromanipulator. This is because the problem turns out to be the design procedure of a single-input single-output, linear time-invariant system that is simple in terms of modelling, controller design, and implementation.

2.2. Mathematical Modelling

Because of the decoupling feature of the proposed micromanipulator, the dynamic behavior of both flexible links can be separately modelled using the same approach. The assumptions and definitions of the micromanipulator's displacements are depicted in **Fig. 2**. The displacement of a flexible link in **Fig. 2(a)** is assumed to take place in just one direction, such as the displacement along the x-axis denoted by x, while the displacement along the z-axis, denoted by z, is ignored because of the small working range, ± 50 μm.

Another important variable is the holding angle denoted by θ in **Fig. 2(b)**. The angle is measured in a downward direction, called a nominal position. The operations of a handheld micromanipulator require the holding angle

to vary $|\theta| \leq 90^\circ$. Such a large variation imposes the complexity of a mathematical model description and hence the design of a controller. For instance, the PWA model is extensively employed in the large parameter variation system.

In this paper, a linear time-invariant model established at the nominal position, $\theta = 0^\circ$, is utilized for a controller design in order to handle the operations of the handheld micromanipulator robustly against large variations in the holding angle. Because each link is constructed from a flexible structure, the dynamic behavior shows strong oscillation and takes a long time to settle whenever the structure is subjected to the external force. Since the working range of each axis is very tiny, a dynamic behavior can be equivalently represented by the standard mass spring damper model (the modeling details are omitted). The linear time-invariant discrete-time state space models for both the x-axis and y-axis are written as

$$\left.\begin{aligned} x(t+1) &= A_x x(t) + B_x u_x(t) \\ z_x(t) &= C_x x(t) + D_x u_x(t) \end{aligned}\right\} \quad \ldots\ldots (1)$$

$$\left.\begin{aligned} y(t+1) &= A_y y(t) + B_y u_y(t) \\ z_y(t) &= C_y y(t) + D_y u_y(t) \end{aligned}\right\} \quad \ldots\ldots (2)$$

where t is a discrete-time index. For the x-axis link, $x \in \mathbb{R}^2$ is a state vector, u_x is an input voltage to corresponding coils, and z_x is an output variable that is the displacement along the x-axis. For the y-axis link, $y \in \mathbb{R}^2$ is a state vector, u_y is an input voltage to corresponding coils, and z_y is an output variable that is the displacement along the y-axis.

3. Robust Hybrid Control for Active Handheld Micromanipulator

The uncertainty caused by large variations in the holding angles results in the robust control framework. The robust hybrid control [30] is extensively studied in the area of MPC in which the dynamic behavior of a system is described by a PWA model, and the MPC controller is designed for such a model. In this paper, a combination of the standard PID controller and the explicit model predictive control is proposed instead. A block diagram of the proposed control scheme for an active handheld micromanipulator, the robust hybrid control, is shown as **Fig. 3**.

The aim of the proposed control scheme is to handle the uncertainty caused by large variations in the holding angle and to achieve a constrained optimal performance. Since the formulation of both the x-axis and y-axis flexible links has the exact same procedure, just the x-axis link will be described.

3.1. PID Controller Design

To investigate the effectiveness of the proposed method, the robust hybrid control scheme is compared to the PID control scheme shown in **Fig. 4**. The variable t in **Fig. 4** represents a continuous time variable. Note that

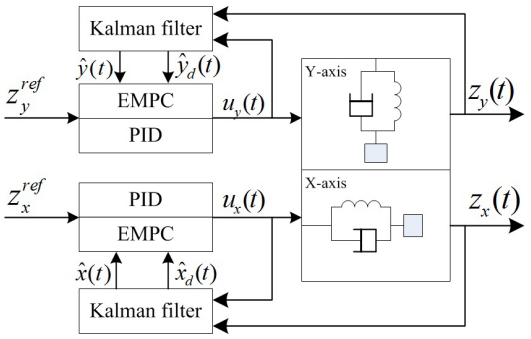

Fig. 3. Hybrid control scheme for a handheld micromanipulator.

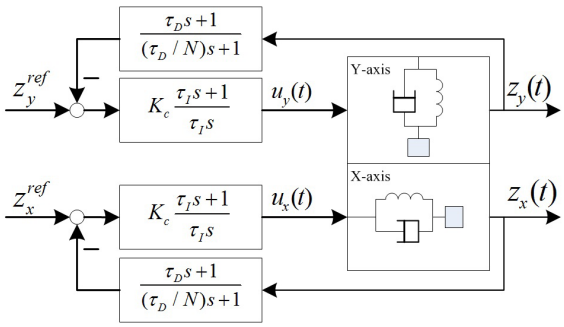

Fig. 4. PID control scheme for handheld micromanipulator.

the robust hybrid control scheme has the PID controller as an ingredient as well. In addition, the same procedure for the computation of PID parameters is employed in both control schemes.

The two degrees of freedom PID controller is utilized; a control law for it is expressed as

$$U_x(s) = \left(K_c \frac{\tau_I s+1}{\tau_I s}\right)\left(z_x^{ref} - \frac{\tau_D s+1}{\left(\frac{\tau_D}{N}\right)s+1} Z_x(s)\right) \quad (3)$$

where K_c, τ_I, τ_D and N are controller parameters which are designed using the tuning rule presented in [31]. The closed-loop time response is specified by tuning value τ_c. Since such tuning rule is based on the standard second-order transfer function with two real poles, the discrete time-state equation in Eq. (1) must be converted to a continuous transfer function and approximated to contain two real poles. Note that the approximation will degrade the performance because the oscillation term is ignored.

3.2. Explicit Model Predictive Control Formulation

The EMPC is utilized as an ingredient of the robust hybrid control in order to optimally compute the input voltage for steering the handheld micromanipulator. To achieve zero steady state error, the problem of offset free tracking is handled by the internal model principle presented in [32] because a linear equality constraint has also been integrated. Although the principle of such an approach guarantees an achievement of zero steady error

when a constant reference is being tracked, the experimental results show that the micromanipulation tasks are satisfied effectively. The standard Kalman filter, additionally, is used to estimate system state variables and disturbances by means of the measurement of the x and y positions.

The ingredients of the EMPC for linear-constrained discrete-time systems consist of:

1) Linear discrete-time model: the linear discrete-time model Eq. (1) that is augmented with the disturbance state x_d at the output is utilized to predict the evolution of the flexible link.

$$\begin{bmatrix} x(t+1) \\ x_d(t+1) \end{bmatrix} = \begin{bmatrix} A_x & 0 \\ 0 & 1 \end{bmatrix} \begin{bmatrix} x(t) \\ x_d(t) \end{bmatrix} + \begin{bmatrix} B_x \\ 0 \end{bmatrix} u_x(t) \quad (4)$$
$$z_x(t) = \begin{bmatrix} C_x & 1 \end{bmatrix} \begin{bmatrix} x(t) \\ x_d(t) \end{bmatrix} + D_x u_x(t)$$

The augmented disturbance state x_d enables the EMPC to achieve the offset free tracking.

2) State and disturbance estimator: for offset-free tracking, state variables are estimated using

$$\begin{bmatrix} x(t+1) \\ x_d(t+1) \end{bmatrix} = \begin{bmatrix} A_x & 0 \\ 0 & 1 \end{bmatrix} \begin{bmatrix} x(t) \\ x_d(t) \end{bmatrix} \begin{bmatrix} B_x \\ 0 \end{bmatrix} u_x(t) + \begin{bmatrix} G_x & 0 \\ 0 & G_{dx} \end{bmatrix} \begin{bmatrix} w_x(t) \\ w_d(t) \end{bmatrix} \quad . \quad . \quad . \quad (5)$$
$$z_x(t) = \begin{bmatrix} C_x & 1 \end{bmatrix} \begin{bmatrix} x(t) \\ x_d(t) \end{bmatrix} + D_x u_x(t) + v_x(t)$$

where $\begin{bmatrix} w_x(t) & w_d(t) \end{bmatrix}^T$ and $v_x(t)$ are assumed to be white Gaussian noise signals. A Kalman filter plays two important roles in the proposed robust hybrid control, which depends on switching policy. If a PID controller is selected, the Kalman filter estimates the current states in order to start the EMPC. If the EMPC is selected, the Kalman filter estimates all states for feedback. The Kalman filter design is accomplished using a MATLAB control system toolbox.

3) Explicit control law synthesis: the main purpose of the handheld micromanipulator is to track the reference signal without steady state error. As a common tracking problem, the quadratic cost function is employed in this paper. The explicit control law [29] is obtained by solving the following optimization problem:

$$\begin{aligned} \min_{u_{x0},\ldots,u_{xN-1}} \quad & \sum_{k=0}^{N-1} \|x_k - \bar{x}_t\|_{Q_x}^2 + \|u_{xk} - \bar{u}_t\|_{R_x}^2 \\ \text{subject to} \quad & E_x x_k + L_x u_{xk} \le M_x, \quad k = 0,\ldots,N \\ & x_{k+1} = A_x x_k + B_x u_{xk}, \quad k = 0,\ldots,N \\ & x_{dk+1} = x_{dk}, \quad k = 0,\ldots,N \quad . \quad . \quad (6) \\ & x_0 = \hat{x}(t) \\ & x_{d0} = \hat{x}_d(t), \end{aligned}$$

in which $\bar{x}_t$ and $\bar{u}_t$ are given by

$$\begin{bmatrix} A_x - I & B_x \\ C_x & 0 \end{bmatrix} \begin{bmatrix} \bar{x}_t \\ \bar{u}_t \end{bmatrix} = \begin{bmatrix} 0 \\ z_x^{ref} - \hat{x}_d(t) \end{bmatrix} \quad . \quad . \quad . \quad (7)$$

where $\|x\|_Q^2 \equiv x^T Q x, Q_x \ge 0$ and $R_x > 0$. The variables $\bar{x}_t$ and $\bar{u}_t$ are the target state and target input, respectively. The constraints, $u_x(t) \le u_x^{max}$ and $z_x(t) \le z_x^{max}$ can be rewritten as the inequality constraint $E_x x_k + L_x u_k \le M_x$, which is presented in the detail in [33]. Note that the current input $u_x(t)$ is distinguished from the optimization variables u_{xk}. Analogously, the state $x(t)$ and $x_d(t)$ denote the system state and disturbance state at time t, while the corresponding variable x_k and x_{dk} denote the predicted state at time $t+k$, obtained by $x_0 = \hat{x}(t)$ and $x_{d0} = \hat{x}_d(t)$.

The optimal control law $u_x^*(t)$ is defined over a polyhedral partition of the state space

$$u_x^*(t) = K_x^i \begin{bmatrix} \hat{x}(t) \\ \hat{x}_d(t) \end{bmatrix} + k_x^i, \quad \begin{bmatrix} \hat{x}(t) \\ \hat{x}_d(t) \end{bmatrix} \in \mathscr{R}^i \quad . \quad (8)$$

The optimal control law Eq. (8) is continuous and piecewise affine in $\begin{bmatrix} \hat{x}(t) & \hat{x}_d(t) \end{bmatrix}^T$. The polyhedral partition is denoted by $\mathscr{R}^i$. The K_x^i and k_x^i are the controller gain corresponding to partition i, or region i. In implementation, the procedure for computing the optimal control law $u_x^*(t)$ consists in determining the active region i which the state variables $\begin{bmatrix} \hat{x}(t) & \hat{x}_d(t) \end{bmatrix}^T$ belongs. Note that the estimated state and disturbance are utilized in the control law. The explicit solutions can be obtained via the multi-parametric toolbox [a] and the searching of the active region can be accomplished by the binary search tree.

3.3. Switching Policy

The proposed robust hybrid control, comprised of the EMPC and PID controller, handles the operations of a handheld micromanipulator constructed from the parallel leaf springs. Such flexible structures inherently produce the blending caused by a gravity force whenever the holding angles are away from the nominal position $\theta = 0^\circ$. The main aim of the PID controller is to bring the flexible link back to center before the EMPC follows the user's commands optimally, such as in circle cutting.

$$\left.\begin{array}{l} \text{if(reference} == 0) \\ \quad \text{PID controller;} \\ \text{else} \\ \quad \text{EMPC;} \\ \text{end} \end{array}\right\} \quad . \quad . \quad . \quad . \quad . \quad . \quad . \quad . \quad . \quad . \quad (9)$$

According to Eq. (9), the reference signal, therefore, is the only factor in the switching policy between the EMPC and PID controller.

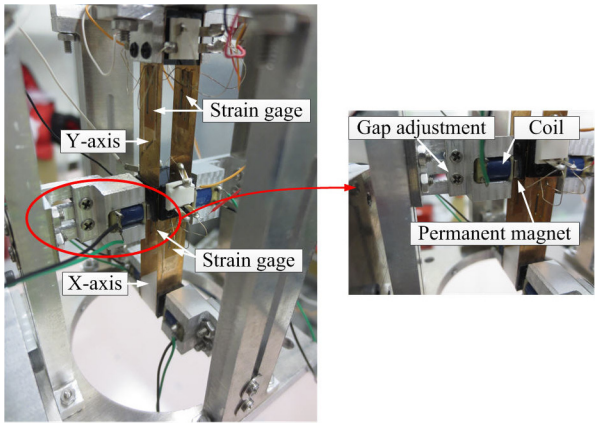

Fig. 5. The experimental setup for micromanipulator prototype.

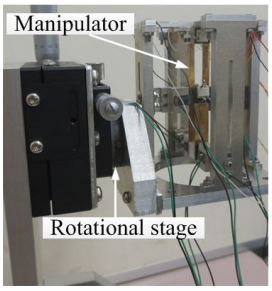

Fig. 6. The experimental setup for holding angle test.

In addition, the current states play a crucial role during the switching period from PID to EMPC control. To smoothly switch, the Kalman filter has to keep estimating all system states, including the disturbance state, even if the handheld micromanipulator is controlled by the PID controller at that time. These estimated states allow for proper and smooth control when the EMPC is switched to. Without information on the current states, the closed-loop system performance becomes poor or even unstable.

4. Experiments

4.1. Experiment Setup

The setup of a micromanipulator experiment is shown in **Fig. 5**. The prototype manipulator consists of two links, the x-axis and y-axis, each of which has the same parallel leaf spring structures 80 μm thick. In addition, the positions of each link are measured by the full bride circuits of strain gauges which have 1928 Ohm gauge resistance, 178 gauge factor, and maximum allowable strain. Each link is steered by double drivings which consist of the combination of coils and permanent magnets, the gaps of which are adjustable. As the primary goal of this system, the gap is set at 100 μm. The setup of the experiment to study the effects of the holding angle is shown in **Fig. 6**. In the experiment, the manipulator is rotated by a rotational stage within $|\theta| \leq 90°$. The control loop is depicted by the simplified block diagram **Fig. 7**. In the control loop, the robust hybrid control is implemented on a desktop PC with

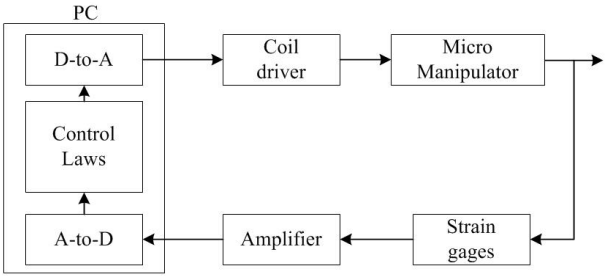

Fig. 7. Simplified block diagram of an experiment setup.

a 3 GHz Intel Core 2 Duo CPU and 4 GB RAM running the Window 7 operating system. The conversion process utilizes the A-to-D and D-to-A PCI-6259 card from National Instrument. The output voltages of the full bridge are amplified by the Kyowa DA-710A module; the signal from it is amplified 200 times.

4.2. Results

The purpose of the experiments is to investigate the reference tracking performance and the effects of holding angle changes under the robust hybrid control. In addition, the results obtained when the robust hybrid control was used are compared to those when the PID control is used.

With a sampling time $T_s = 0.001$ second, the dynamic behavior of the x-axis and y-axis flexible links can be roughly identified and described by the discrete-time state spaces in Eqs. (1) and (2) with

$$A_x = \begin{bmatrix} 0.9434 & 0.3143 \\ -0.3163 & 0.9490 \end{bmatrix}, \quad B_x = \begin{bmatrix} 0.0004 \\ 0.0149 \end{bmatrix}$$
$$C_x = \begin{bmatrix} 498.1674 & 57.1028 \end{bmatrix}, \quad D_x = 0 \quad . \quad . \quad . \quad (10)$$
$$A_y = \begin{bmatrix} 0.9769 & 0.1649 \\ -0.1653 & 0.9845 \end{bmatrix}, \quad B_y = \begin{bmatrix} 0.0007 \\ 0.0106 \end{bmatrix}$$
$$C_y = \begin{bmatrix} 543.0023 & 36.6877 \end{bmatrix}, \quad D_y = 0. \quad . \quad . \quad . \quad (11)$$

where the identifications are accomplished by the system identification toolbox by means of estimating model parameters using the iterative prediction-error minimization method, or PEM. The identifying performance is measured by

$$\text{Fit} = 100 \left(1 - \frac{\|s - m\|_2}{\|m - \bar{m}\|_2} \right) \quad . \quad . \quad . \quad . \quad . \quad . \quad . \quad . \quad (12)$$

where m and $\bar{m}$ are the measured output and its mean, respectively, whereas s is the results when the model is simulated with the corresponding input. As a result, the identifying performances of the x- and y-axis Eqs. (10) and (11) achieves the 97.53% and 93.44% Fits, respectively.

In order to design the PID parameters according to the tuning rule presented in [31], the models in Eqs. (10) and (11) have to be converted and approximated again by a continuous transfer function with two real poles. As a result, the PID parameters for both the x- and y-axis are shown in **Table 1**. For the EMPC design, the prediction

Table 1. PID parameter values for X-axis and Y-axis links.

Link	K_c	τ_I	τ_D	N
X	$6.928 * 10^{-4}$	0.0016	0.0016	100
Y	$6.651 * 10^{-4}$	0.023	0.023	100

and control horizon chosen are 10 and 2, respectively. The multiparametric toolbox [a] is used to solve the problem in Eq. (6) and synthesize the associated controller, which results in 55 regions for the x-axis link and 43 regions for the y-axis link. The difference comes from different dynamics.

For the Kalman filter design, the augmented model in Eq. (5) is directly used with the given matrices in Eqs. (10) and (11). The matrices $G_x = \begin{bmatrix}0.0012 & 0.0014\end{bmatrix}^T$ and $G_{dx} = 10$ are utilized for the x-axis link whereas the matrices $G_y = \begin{bmatrix}0.0014 & 0.005\end{bmatrix}^T$ and $G_{dy} = 10$ are utilized for the y-axis link. In the experiments, we found that the matrices G_{dx} and G_{dy} had a profound effect on the estimating time of the states $x_d(t)$ and $y_d(t)$. Therefore, the matrices G_{dx} and G_{dy} could be considered as the performance tuning parameter. In addition, based on trial and error, the variances selected are $E[w_x w_x^T] = E[w_y w_y^T] = 0.001$, $E[v_x v_x^T] = E[v_y v_y^T] = 0.01$ and $E[w_d w_d^T] = 0.01$ for both links.

There are two types of reference signals used in the experiments, i.e., step and sinusoidal signals. The amplitude of the step signal is 50 μm and tracking is excited at 1 second.

For a circle, the following reference signals are utilized

$$\left.\begin{aligned} z_x^{ref} &= m_x \cos(2\pi f t) \\ z_y^{ref} &= m_y \sin(2\pi f t) \end{aligned}\right\} \quad \cdots\cdots\cdots \quad (13)$$

The frequency $f = 2$ Hz, which is reasonable in practice, and magnitudes $m_x = m_y = 50$ μm are used for tracking a circle. Generally, the amplitude can be any value in the working range. Both step and sine tracking tasks are conducted at the angles $\theta = 0^\circ, 30^\circ, 60^\circ, 90^\circ$ and -90°.

4.3. Robust Tracking Performance

In **Fig. 8**, the closed-loop responses of the handheld micromanipulator controlled by the robust hybrid control can be seen. While varying the holding angle for the x-axis, we try to maintain $\theta = 0$ for the y-axis. The holding angle has a strong effect on the initial positions $z_x(0)$ and $z_y(0)$. For instance, the initial positions become zeros when $\theta = 0^\circ$ because there is no bending caused by the force of gravity. Thus, two links are in the center. For $\theta = 90^\circ$, the initial positions of the x-axis and y-axis are $z_x(0) = 105$ μm and $z_y(0) = 5$ μm. Each link is away from the center, especially the x-axis. Due to the parallel leaf spring structure in cascade, the difference in the initial positions is affected by the bending and blocking state of each flexible link. In this case, the x-axis link

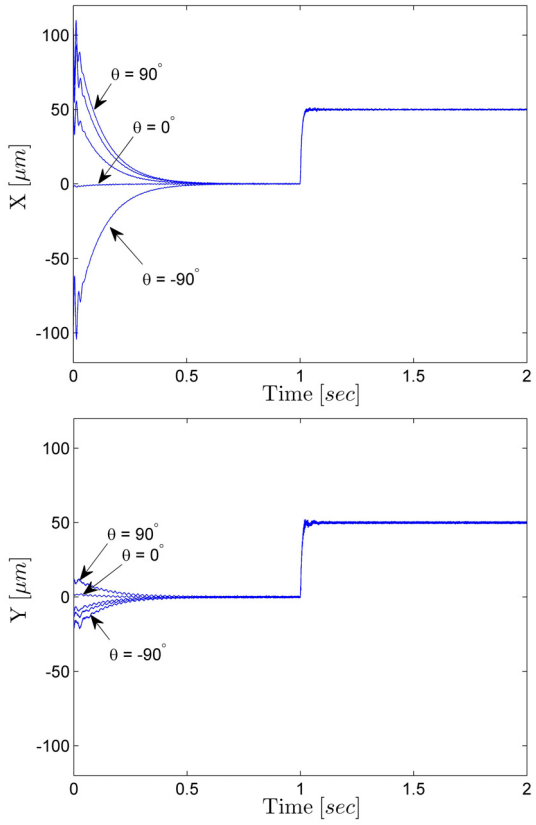

Fig. 8. Step responses under the holding angle changes.

is in the bending state whereas the other is in the blocking state. We see that the responses of the x- and y-axes are brought back to the center in 0.5 second for all holding angle changes, which is reasonable in practice: the user has to wait only 0.5 second before starting the tracking process. During this time, the reference signal must obviously be zero, which means the micromanipulator is controlled by the PID controller. The experiments show that the holding angle changes in the interval $|\theta| \leq 90^\circ$ are handled successfully.

The reference signals $z_x^{ref} = 50$ μm and $z_y^{ref} = 50$ μm are initiated at 1 second. Because of reference signals are non-zero, the robust hybrid control switches to the EMPC to optimally track the reference signal. Both x-axis and y-axis responses achieve good, robust tracking performance, as shown in **Fig. 8**. Only 0.05 second is required for all variations of the holding angle in the specified interval to reach the target. Additionally, the steady state responses contain very little fluctuation in a tracking phase. Although the fluctuation takes place on the y-axis during the transient response, such fluctuation is less than 4 μm. Thus, the results of the experiment have confirmed robust step tracking performance.

Figure 9 presents the results of the experiment to track the circle reference signal. The holding angle was changed in the interval $|\theta| \leq 90^\circ$. The plots show only the tracking phase; in other words, the interval time utilized to bring both flexible links back to the center has been removed. The experiments show that the circle tracking

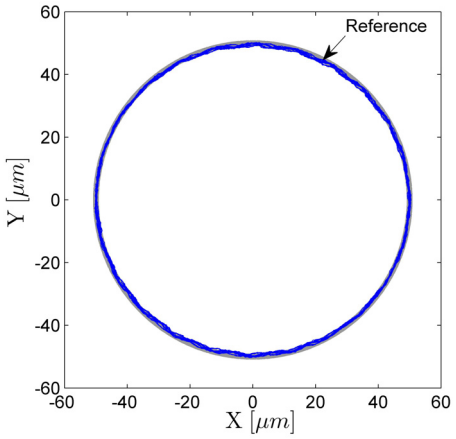

Fig. 9. Circle tracking at holding angles of $\theta = 0°, 30°, 60°, 90°$ and $-90°$.

task was completed satisfactorily with fluctuations under 2 μm.

In conclusion, the experimental results indicate that the proposed handheld micromanipulator with the proposed robust hybrid control achieves not only fast transient response with little fluctuation but also robustness against holding angle changes.

4.4. Comparison to PID Controller

The PID controller is utilized to control the handheld micromanipulator in order to show the effectiveness of the proposed robust hybrid control and demonstrate that the PID controller with a standard tuning rule is unable to achieve an acceptable level of tracking performance. The comparisons of tracking step and sinusoidal reference signals are shown only at the holding angle $\theta = 60°$ because we obtained the same results at the other angles.

In **Fig. 10**, the differences in when the handheld micromanipulator is controlled by the robust hybrid control and by the PID controller are shown. The step signals with the amplitude 50 μm initiated at 1 second are used as the reference signal. We see that both controllers are able to bring the micromanipulator back to the center because the PID controller in the robust hybrid control becomes active in this period, giving exactly the same results. The reference changes to 50 μm from 1 second. For the robust hybrid control, the EMPC becomes active and follows the reference perfectly. There is a big difference from the tracking phase; the time response of the PID controller is ten times slower than it is in the proposed method. Both controllers are able to have no steady state error and the very little fluctuation, less than 1 μm at a steady state. The corresponding control signals are shown in **Fig. 11**. Note that the robust hybrid control results in similar responses for the x- and y-axis, and such similarity is preferable. The PID controller produces the same similarity as well.

In **Fig. 12**, the disturbance states $x_d(t)$ and $y_d(t)$ estimated by the Kalman filter are shown. The estimated states include the uncertainties caused by unmodelled dynamic and model mismatch due to the holding angle

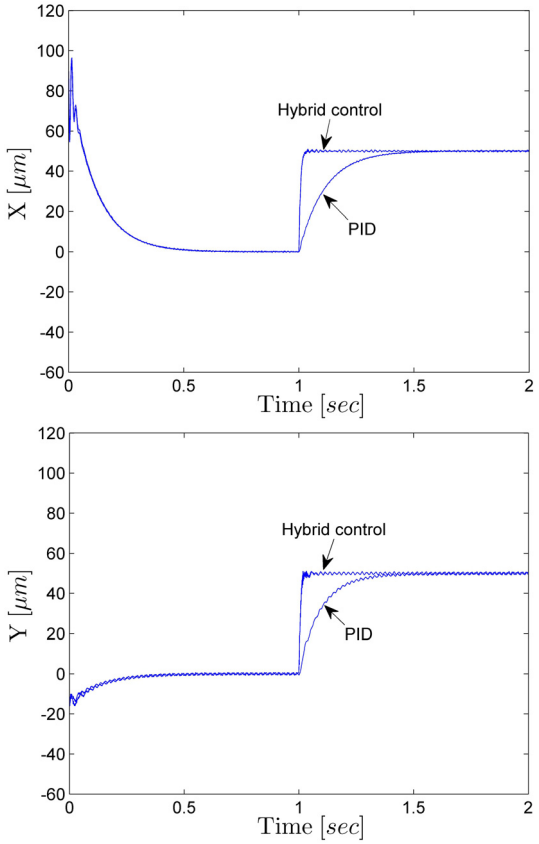

Fig. 10. Comparison at the holding angle $\theta = 60°$ of a step response with amplitude 50 μm initiated at 1 second.

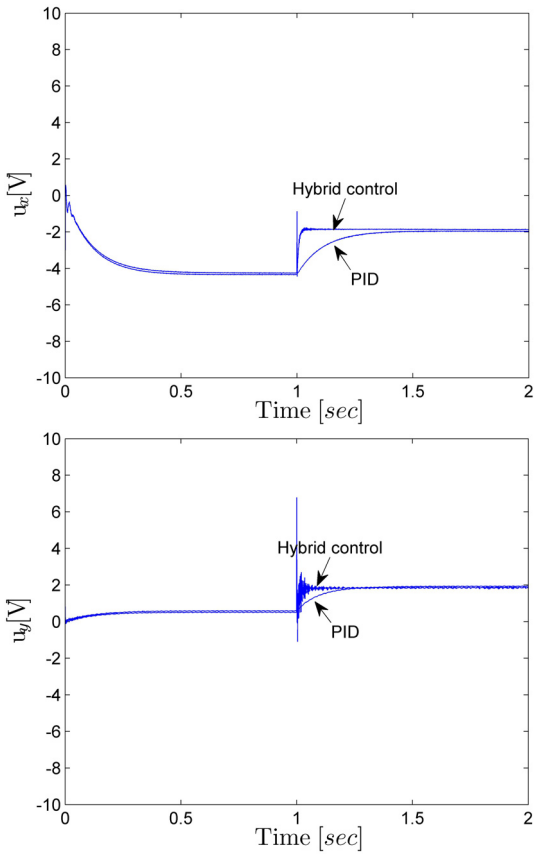

Fig. 11. Control signals due to a step signal reference with an amplitude of 50 μm initiated at 1 second at $\theta = 60°$.

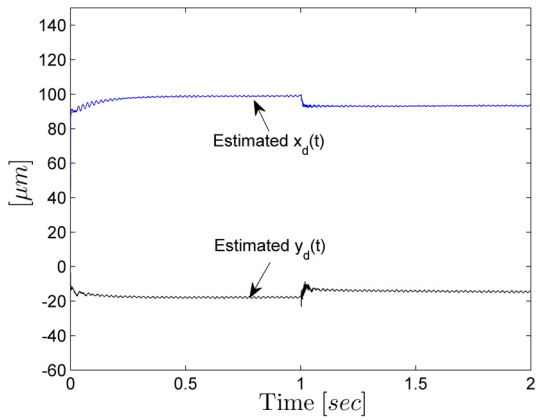

Fig. 12. Disturbance states estimated by the Kalman filter at the holding angle $\theta = 60°$.

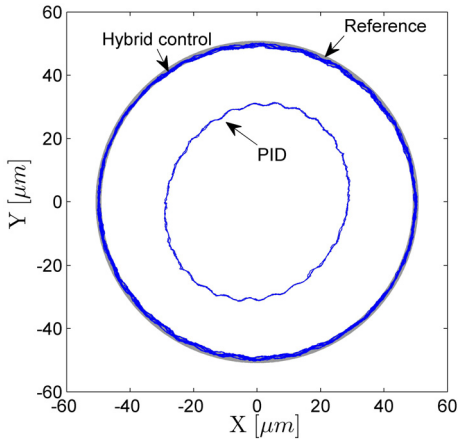

Fig. 13. Comparison of a circle tracking with 50 μm radius at the holding angle $\theta = 60°$.

changes. The initial positions at $\theta = 60°$ are $z_x(0) = 90$ μm and $z_y(0) = -10$ μm.

To compare frequency responses, the ability to make a circle with a 50 μm radius was investigated by employing the reference signals in Eq. (13). The results obtained are shown in **Fig. 13**. Obviously, the PID controller failed to follow the reference because of the narrow bandwidth, whereas the proposed method completed the circle reference with less than 2 μm of fluctuation. However, a frequency lower than 0.2 Hz allowed the PID controller to track the circle with an acceptable level of fluctuation, 6 μm.

The experimental comparisons have revealed that the standard PID controller failed to reach the requirements of the handheld micromanipulator. However, the strength of the PID controller is its ability to bring the flexible links back to center, which motivates authors to integrate the PID controller into the proposed robust hybrid control.

5. Discussion

We have shown that a high-performance handheld micromanipulator can be created with a simple design in

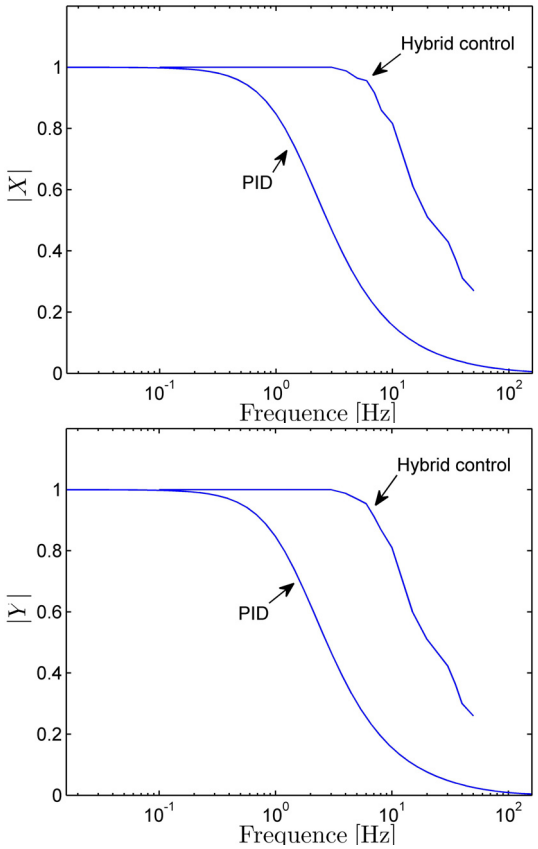

Fig. 14. Comparison of frequency responses.

terms of the structure and mathematical model. Since the PID controller fails to meet the requirements, we have proposed a robust hybrid control. Experiments have shown that the robust hybrid control produces satisfactory results. The ability to track a circle with a 50 μm radius in 0.5 seconds in practice is sufficiently fast. In addition, the micromanipulator requires 0.5 seconds to start at any operating angle just to set center. This time may be reduced by redesigning the PID controllers. The closed-loop time constant τ_c selected for this paper is the smallest value that results in the fastest stable system, based on the tuning rule presented in [31]. Larger values cause the handheld micromanipulator to be unstable. The limitation in employing the tuning rule comes from the fact that the under damp second order system is approximated by two real poles.

We have imitated the application of the handheld micromanipulator by changing the holding angle $|\theta| \leq 90°$, which covers the full range in practice. Several experiments, in which both step and sinusoidal signal references were studied, were conducted to confirm its robust performance. The results shown in **Figs. 8** and **9** guarantee the effectiveness of the proposed approach. The handheld micromanipulator can track other shapes, such as ellipsoids, for which the amplitude m_x and m_y are different.

A comparison of frequency responses is shown in **Fig. 14**. The frequency responses of the hybrid control were obtained in experiments in which the system was operated without any constraints. Obviously, the hybrid

control achieves a wider bandwidth, 8.5 Hz, than does the PID controller. The bandwidth achieved is capable of handling fluctuations with a frequency of around 10–13 Hz caused by the user's hand [34]. Moreover, the bandwidth can be reduced to 2.5 Hz to effectively handle such fluctuations and be fast enough to accomplish tracking tasks. However, in all experiments we presented in this paper, the handheld micromanipulator was fixed on the rotational stage in order to study the effects of holding angle changes only. Fluctuations caused by the user's hand should be studied as well. This is considered as the future work with a view to making the active handheld micromanipulator more suitable for practical application.

6. Conclusion

We have proposed a handheld micromanipulator controlled by the robust hybrid control. In this control, the EMPC and PID controller are combined and called robust hybrid control. The switching mechanism is based on the fact that the Kalman filter estimates the current states and passes from the PID controller to the EMPC. The main aim of the proposed robust hybrid control is to produce robustness against changes in the holding angle. The effectiveness of the micromanipulator has been demonstrated by comparing its experimental results to those of a PID controller. The results have shown that robust tracking performance was successfully achieved.

References:

[1] H. Das, H. Zak, J. Johnson, J. Crouch, and D. Frambach, "Evaluation of a telerobotic system to assist surgeons in microsurgery," Computer Aided Surgery, Vol.4, No.1, pp. 15-25, 1999.

[2] Y. M. Baek, Y. Kozuka, N. Sugita, A. Morita, S. Sora, R. Mochizuki, and M. Mitsuishi, "Highly precise Master-Slave Robot System for Super Micro Surgery," In Proc. the 2010 3rd IEEE RAS & EMBS Int. Conf. Bio. Robot. and Biomechatronics, Japan, Sep. 2010.

[3] R. Kumar, P. Jensen, and R. H. Tayor, "Experiments with a Steady Hand Robot in Constrained Compliant Motion and Path Following," in Proc. IEEE Int. on Robot and Human Interaction, Italy, Sep. 1999.

[4] A. Bettini, P. Marayong, S. Lang, A. M. Okamura, and G. D. Hager, "Vision-Assisted Control for Manipulation Using Virtual Fixtures," IEEE Trans. Robot., Vol.20, No.6, pp. 953-966, 2004.

[5] B. Bose, A. Kalra, S. Thukral, A. Sood, S. Guha, and S. Anand, "Tremor compensation for robotics assisted microsurgery," Engineering in Medicine and Biology Society, 1992 14th Annual IEEE Int. Conf., Vol.3, pp. 1067-1068, 1992.

[6] D. Y. Choi and C. N. Riviere, "Flexure-based Manipulator for Active Handheld Microsurgical Instrument," in Proc. IEEE Engineering in Medicine and Biology 27th Annual Conf., China, pp. 5085-5088, Sep. 2005.

[7] W. T. Latt C. Y. Shee, and W. T. Ang, "A Compact Handheld Active Physiological Tremor Compensation Instrument," 2009 IEEE/ASME Int. Conf. on Advanced Intelligent Mechatronics, Singapore, pp. 711-716, July 2009.

[8] S. Yang, R. A. MacLachlan, and C. N. Riviere, "Design and Analysis of 6 DOF Handheld Micromanipulator," 2012 IEEE Int. Conf. Robot. Autom., USA, pp. 1946-1951, May 2012.

[9] R. A. MacLachlan, B. C. Becker, J. C. Tabarés, G. W. Podnar, L. A. Lobes, Jr., and C. N. Riviere, "Micron: An Actively Stabilized Handheld Tool for Microsurgery," IEEE Trans. Robot., Vol.28, No.1, pp. 195-212, 2012.

[10] S. Skogestad and L. Postletwaite, "Multivariable Feedback Control: Analysis and Design," 2nd Edition, John wiley & Sons, 2005.

[11] L. J. Everett, J. Tang, and M. Compere, "Designing Flexible Manipulators with the Lowest Natural Frequency Nearly Independent of Position," IEEE Trans. Robot., Vol.15, No.4, pp. 605-611, 1999.

[12] T. Fukuda, H. Sato, F. Arai, H. Iwata, and K. Itoigawa, "Parallel Beam Micro Sensor/Actuator Unit Using PZT Thin Films and Its Application Examples," in Proc. IEEE Int. Conf. Robot. Autom., Leuven, Belgium, pp. 1498-1503, May 1998.

[13] H. Sato, T. Fukuda, F. Arai, K. Itoigawa, and Y. Tsukahara, "Suppression of Mechanical Coupling for Parallel Beam Gyrscope," in Proc. IEEE Int. Conf. Robot. Autom., San Francisco, pp. 3939-3944, April 2000.

[14] C. E. García, D. M. Prett, and M. Morari, "Model Predictive Control: Theory and Practice – a Survey," Automatica, Vol.25, No.3, pp. 335-348, 1989.

[15] M. Morari and J. H. Lee, "Model Predictive Control: Past, Present and Future," Computers and Chemical Engineering, Vol.23, pp. 667-682, 1999.

[16] A. Bemporad and M. Morari, "Robust Model Predictive Control: A Survey," J. Robustness in Identification and Control, Vol.245, pp. 207-226, 1999.

[17] D. Q. Mayne, J. B. Rawlings, C. V. Rao, and P. O. M. Scokaert, "Constrained Model Predictive Control: Stability and Optimality," Automatica, Vol.36, pp. 789-814, 2000.

[18] J. M. Maciejowski, "Predictive Control with Constraints," Englewood Cliffs, NJ: Prentice-Hall, 2002.

[19] S. Qin and T. Badgwell, "A survey of Industrial Model Predictive Control Technology," Control Engineering Practice, Vol.11, pp. 733-764, 2003.

[20] A. Aswani, J. Taneja, and C. Tomlin, "Reducing Transient and Steady State Electricity Consumption in HVAC Using Learning-Based Model Predictive Control," Proc. IEEE, Vol.100, No.1, pp. 240-253, 2012.

[21] F. Oldewurtel, A. Parisio, C. N. Jones, D. Gyalistras, M. Gwerder, V. Stauch, B. Lehmann, and M. Morari, "Use of Model Predictive Control and Weather Forecasts for Energy Efficient Building Climate Control," Energy and Building, Vol.45, pp. 15-27, 2012.

[22] S. Bolognani and L. Peretti, "Design and Implementation of Model Predictive Control for Electrical Motor Drives," IEEE Trans. Ind. Electron., Vol.56, No.6, pp. 1925-1936, 2009.

[23] S. Mariéthoz, A. Domahidi, and M. Morari, "High-Bandwidth Explicit Model Predictive Control of Electrical Drives," IEEE Trans. Ind. Appl., Vol.48, No.6, pp. 1980-1992, 2012.

[24] D. Hrovat, S. Di Cairano, H. E. Tseng, and I. V. Kolmanovsky, "The Development of Model Predictive Control in Automotive Industry: A Survey," in Proc. IEEE Int. Conf. Cont. Appl., Dubrovnik, Croatia, October 3-5, 2012.

[25] M. Hassan, R. Dubay, C. Li, and R. Wang, "Active Vibration Control of a Flexible One-Link Manipulator using a Multivariable Predictive Controller," Mechatronics, Vol.17, pp. 311-323, 2007.

[26] A. G. Wills, D. Bates, A. J. Fleming, B. Ninness, and S. O. R. Moheimani, "Model Predictive Control Applied to Constraint Handling in Active Noise and Vibration Control," IEEE. Trans. Control Syst. Technol., Vol.16, No.1, pp. 3-12, 2008.

[27] P. Boscariol, A. Gasparetto, and V. Zanotto, "Model Predictive Control of a Flexible Links Mechanism," J. Intell Robot Syst., Vol.58, pp. 125-147, 2010.

[28] S. Boksuwan and T. Benjanarasuth, "Robust Real-time Model Predictive Control for Torsional Vibration System," Int. J. Automation Tech., Vol.6, No.3, 2012.

[29] A. Bemporad, F. Borrelli, and M. Morari, "Model predictive control based on linear programming the explicit solution," IEEE Trans. Autom. Control, Vol.47, pp. 1974-1985, 2002.

[30] M. Kvasnica, "Real-Time Model Predictive Control via Multi-Parametric Programming: Theory and Tools," VDM Verlag Dr. Müller, 2009.

[31] S. Skogestad, "Simple Analytic Rule for Model Reduction and PID Controller Tuning," J.of Process Control, Vol.13, pp. 291-309, 2003.

[32] U. Macder, F. Bomelli, and M. Morari, "Linear offset-free Model Predictive Control," Automatica, Vol.45, pp. 2214-2222, 2009.

[33] A. Bemporad, M. Morari, V. Dua, and E. N. Pistikopoulos, "The Explicit Linear Quadratic Regulator for Constrained Systems," Automatica, Vol.38, pp. 3-20, January 2002.

[34] R. A. MacLachlan, B. C. Becker, G. W. Podnar, L. A. Lobes, and C. N. Riviere, "Micron: An actively Stabilized Handheld Tool for Microsurgery," IEEE Trans. Robotics, Vol.28, No.1, pp. 195-212, 2012.

Supporting Online Materials:

[a] M. Kvasnica, P. Grieder, M. Baotic, and M. Morari, "Multi-parametric Toolbox (MPT)." http://control.ee.ethz.ch/~mpt/ [Accessed October 9, 2012]

Name:
Sungwan Boksuwan

Affiliation:
Ph.D. Student, Department of Mechanical Engineering and Intelligent System, The University of Electro-Communications

Address:
1-5-1 Chofugaoka, Chofu-shi, Tokyo 182-8585, Japan

Brief Biographical History:
2007- Joined Faculty of Engineering, King Mongkut's Institute of Technology Ladkrabang
2012- Visiting Researcher, Norwegian University of Science and Technology (NTNU)

Main Works:
• "Robust Real-Time Model Predictive Control for Torsional Vibration System," Int. J. of Automation Technology, Vol.6 No.3, 2012.

Name:
Taworn Benjanarasuth

Affiliation:
Associate Professor, Faculty of Engineering, King Mongkut's Institute of Technology Ladkrabang

Address:
1 Chalongkrung Soi 1, Ladkrabang, Bangkok 10520, Thailand

Brief Biographical History:
1996- Joined Faculty of Engineering, King Mongkut's Institute of Technology Ladkrabang

Main Works:
• "New Tuning Formulas for Two-Degree of Freedom PID Controllers and the Application to Level Control Systems," The Trans. of the Institute of Electrical Engineering of Japan (IEEJ) on Industry Applications, Vol.127, No.5, 2007.

Membership in Academic Societies:
• The Institute of Electrical and Electronics Engineers (IEEE)
• Engineering/Electronics, Computer, Telecommunications and Information Technology Association of Thailand (ECTI)

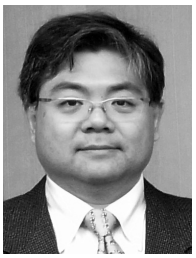

Name:
Chisato Kanamori

Affiliation:
Associate Professor, Department of Mechanical Engineering and Intelligent Systems, Graduate School Informatics and Engineering, The University of Electro-Communications

Address:
E4-303, 1-5-1 Chofugaoka, Chofu-shi, Tokyo 182-8585, Japan

Brief Biographical History:
1987 Received B.E. from The University of Electro-Communications
1989 Received M.E. from The University of Electro-Communications
1991- Research Associate, The University of Electro-Communications
2004 Received D.E. from The University of Electro-Communications
2005- Associate Professor, The University of Electro-Communications

Main Works:
• J. Kitawaki and C. Kanamori, "Development of Intelligent Encoder," Proc. of The Twenty-third Annual Meeting of The American Society for Precision Engineering and the Twelfth ICPE (CD-ROM), #2639, p. 4, Portland, USA, Oct. 21, 2008.
• C. Kanamori, M. Kajitani, and M. Shimojo, "Development of 3-D Coordinate Measuring System Using Laser Plane Scanners," First Asia Int. Symposium on Mechatronics (AISM2004), PJ 26, Sep. 2004.

Membership in Academic Societies:
• The Japan Society of Mechanical Engineers (JSME)
• The Japan Society of Precision Engineering (JSPE)
• The Robotics Society of Japan (RSJ)

Name:
Hisayuki Aoyama

Affiliation:
Professor, Department of Mechanical Engineering and Intelligent Systems, The University of Electro-Communications

Address:
E4-303, 1-5-1 Chofugaoka, Chofu-shi, Tokyo 182-8585, Japan

Brief Biographical History:
1983- Research Laboratory of Precision Machinery and Electronics, Tokyo Institute of Technology
1988- Department of Precision Engineering, Shizuoka University
1997- Department of Mechanical Engineering and Intelligent Systems, The University of Electro-Communications

Main Works:
• "Precise miniature robots and desktop flexible production," Proc. of Int. Workshop on Micro Factory, pp. 149-156, 1998.

Membership in Academic Societies:
• The Japan Society of Mechanical Engineers (JSME)
• The Japan Society of Precision Engineering (JSPE)
• The Robotics Society of Japan (RSJ)
• American Society for Precision Engineering (ASPE)